ANZIAM J. 57(2015), 175–188
doi:10.1017/S1446181115000206

BATCH PROCESSING IN A GLASS FURNACE

NEVILLE D. FOWKES[✉1] and ANDREW P. BASSOM[1,2]

(Received 7 May, 2015; accepted 25 July, 2015; first published online 2 October 2015)

Abstract

In a glass furnace solid batches of material are fed into a chamber and radiation heating applied. An individual batch is melted over the course of several minutes to form molten glass. A travelling front within the batch designates the progress of the melting, a process characterized by multiple radiation reflections. This results in an effective conductivity within the melting zone that is significantly larger than that in the unmelted batch. Approximations based on these disparate conductivities enable accurate explicit expressions for the almost constant melting front speed and the associated temperature profile to be derived. Our results compare favourably with existing numerical simulations of the process, with the advantage of being both analytic and relatively simple. These predictions may be useful in suggesting how a furnace might be most effectively controlled under varying batch conditions, as well as ensuring the quality of the glass sheets produced.

2010 *Mathematics subject classification*: 80.

Keywords and phrases: glass furnace, melting front, radiative heating, asymptotics.

1. Introduction

Glass furnaces are complex pieces of equipment that typically need to operate continuously over the lifetime of a factory in order to avoid catastrophic glass solidification. Ongoing careful monitoring is essential to ensure the quality of the final product, and this necessitates understanding the chemical and physical processes occurring within the furnace. Here our interest will principally be with the latter, but in order to make headway, it is important to note some basic chemistry; the most fundamental fact we need to remember is that the main component of glass is silica (SiO_2), which under natural conditions occurs as sand. The silica structure consists of strong SiO_4 tetrahedra joined by chemical bridges. When a suitable fluxing material is added to the crystalline material, it breaks the bridges, leading to a weaker interaction between the silicon atoms. This modifies the network and results in the transparent

[1]School of Mathematics and Statistics, University of Western Australia, Crawley, WA 6009, Australia; e-mail: neville.fowkes@uwa.edu.au.
[2]School of Mathematics & Physics, University of Tasmania, Private Bag 37, Hobart, TAS 7001, Australia; e-mail: andrew.bassom@utas.edu.au.

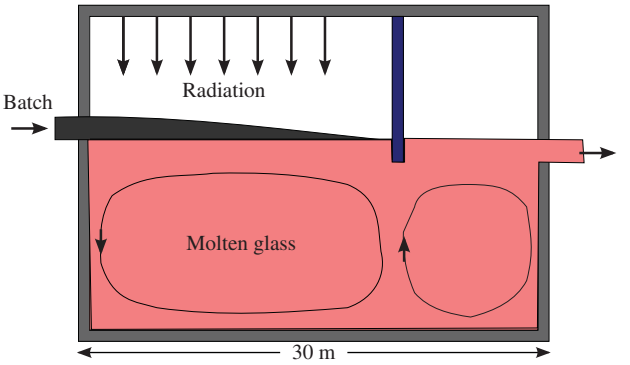

FIGURE 1. Diagram of a glass furnace. Radiative heating from ceiling flames together with direct heating from combustion gases melt the floating batch. Molten glass overflows into a second chamber to the right.

substance we recognize as glass. The reaction is endothermic and can only occur at high temperatures.

In a typical industrial furnace, a solid batch of material, consisting principally of ground silica of depth of a few centimetres, is fed at a speed of about $1\,\mathrm{m\,s^{-1}}$ into the furnace. The chamber, which may be as large as 30 m long, 10 m wide and 4 m high, contains about 1000 tonnes of already molten glass as shown in Figure 1. The incoming batch floats on top of the molten glass. The batch material is guided into the furnace by a moving barrier which has the effect that the batch enters in distinct mounds rather than as a continuous feed. After entry the floating layer often splits into two separate piles attached to the side walls of the furnace, and radiation from flames located at the top of the furnace gradually melts the batch, thereby yielding liquid glass. The floating layers of the input batch extend approximately 20 m into the furnace before they are completely melted. Typical temperatures of the molten glass are of the order of 1500 °C, and particles stay within the molten glass bath for about 10–15 h. The excess glass in the furnace overflows into a second chamber where the temperature is reduced to about 1400 °C, which is the appropriate temperature for glass production using the Pilkington tin float process, now described. The molten glass from the second chamber is fed onto a long tray of depth 0.5 m and width 7 m containing molten tin of depth a few centimetres. The liquid glass spreads out over the molten tin, forming a sheet (typically 7–10 mm thick) which solidifies as it travels along, and is drawn off as a solid glass sheet which is subsequently cut into appropriate sizes. More details of the operation of a furnace can be found in any of the articles [1, 4, 10], while an excellent mathematical analysis of the whole process is given by Howell [3].

Our concern here is with the development of a simplified mathematical model of the melting of the batch which does not require us to delve into the complications of the underlying chemistry. We shall consider an idealized batch of uniform thickness that is introduced into a furnace at a constant speed and which floats on top of previously

https://doi.org/10.1017/S1446181115000206 Published online by Cambridge University Press

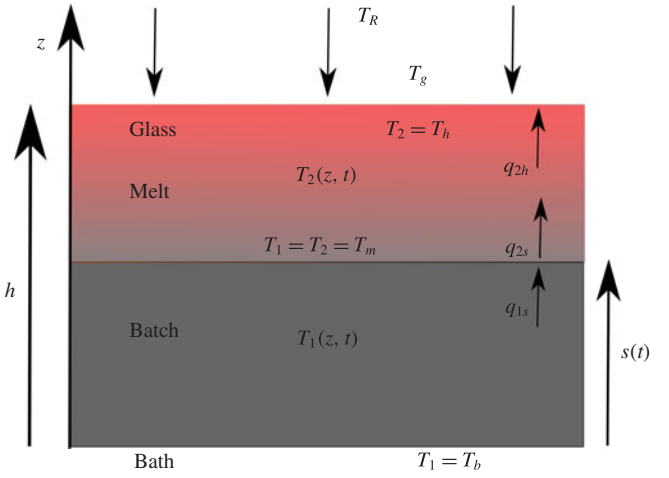

FIGURE 2. The melting of an element of the batch. Two distinct regions are separated by a front located at $z = s(t)$: the lower zone $z < s(t)$ consists of unmelted batch, and the upper region $z > s(t)$ contains melted or partially melted batch.

melted glass. Radiation from the flames above increases the temperature of the batch, and melting commences at its uppermost surface when its temperature achieves the melting value (1123 K). Depending on morphology and surface tension characteristics of the freshly formed melted glass, it will either remain on the surface or may drain over the top of the batch or through the batch.

In order to develop and analyse the model, the remainder of the paper is organized in the following manner. Presently, in Section 2, we elaborate on the details of the model summarized in the preceding paragraph and derive a simple but nonetheless accurate description of the problem. Some asymptotic solutions are derived in Section 3, and our studies conclude with some remarks in Section 4.

2. Development of the model

Our model consists of an element of the batch which is supposed to be of depth h. With the coordinate z measured vertically upward from the surface of the already melted glass, the batch occupies the region $0 < z < h$ and at time $t = 0$ enters the furnace. The batch begins to melt from its top and when $t > 0$ the extent of the melt has descended to the front at $z = s(t)$; see Figure 2. This front divides the batch into two zones. In the lower zone, $z < s(t)$, which we will designate zone 1, the batch is still intact. In the upper zone, $s(t) < z < h$ (zone 2), melting is either complete or under way, so that this zone consists of a mixture of solid and melted particles. The flame at the top of the furnace is supposed to radiate at an effective temperature T_R, whilst the upper surface of the batch is bathed in gas at temperature T_g.

Roughly 80% of the emitted radiation at temperature T_R intercepts the batch and is absorbed; the remainder is reflected or lost to the environment. At the location z

https://doi.org/10.1017/S1446181115000206 Published online by Cambridge University Press

within the melting region (zone 2), the incoming radiation that intercepts intact sand particles will partially reflect and absorb; in particular, no radiation will be transmitted through the sand. On the other hand, any already (partially) melted glassy component is semi-transparent to incoming radiation and, thus, incident radiation passes through this layer to be absorbed and reflected at lower levels. Some of the secondary reflections from lower levels will intercept sand particles, resulting in tertiary reflections and absorptions and associated melting. Moreover, the sand particles and the heated glass will re-radiate in all directions and conduction will transfer heat between layers. Any bubbles produced within the melting batch will also act as scatterers of radiation, especially within the glassy upper layers. There will be a layer of pure glass (completely converted batch) at the top, $z = h$, with the fraction of batch that has been melted falling as z decreases to the front at $s(t)$.

The field equations (known as the semi-transparent batch model) for the temperatures in the two regions $(T_1(z,t), T_2(z,t))$ were derived by Wu and Viskanta [11]. If the densities, specific heats and conductivities within the two zones are denoted by (ρ_i, c_i, k_i), for $i = 1, 2$, then

$$\rho_1 c_1 \frac{\partial T_1}{\partial t} = \frac{\partial}{\partial z}\left(k_1(T)\frac{\partial T_1}{\partial z}\right) \quad \text{for } z < s(t),$$
$$\rho_2 c_2\left[\frac{\partial T_2}{\partial t} + \left\{\left(1 - \frac{\rho_1}{\rho_2}\right)\frac{ds}{dt}\frac{\partial T_2}{\partial z}\right\}\right] = \frac{\partial}{\partial z}\left(k_2(T)\frac{\partial T_2}{\partial z}\right) - \frac{\partial F}{\partial z} + H_2 \quad \text{for } z > s(t).$$

In the second equation, $F(z,t)$ denotes the total radiative flux, and $H_2(z,t)$ is the (local) enthalpy change due to melting. The bracketed term $\{\cdot\}$ on the left-hand side of the second equation takes into account the volumetric change associated with the moving front. Boundary conditions need to be specified at the bottom $z = 0$ and top $z = h$ of the batch, and state change (Stefan) conditions applied at the front $s(t)$.

The specific heats c_i are temperature invariant within the individual regions but take different values in the two zones, so $c_1 \neq c_2$. The density within the melt is a function of the degree of conversion that has taken place and, although it affects the position of the upper surface of the melt relative to a fixed frame, it does not play a role in fixing the front speed so will be treated as a constant here. Unfortunately, though taking the specific heats and densities as constants is a reasonable approximation, the same cannot be said for the conductivities which strongly vary with the temperature. The conductivity of sand increases exponentially by a factor of about 2 over the relevant temperature range of interest, and experiments described by Schick et al. [7] and Shibata et al. [8] suggest that

$$k_1(T) = k_{10}\exp\left(\gamma\left(\frac{T}{T_0} - 1\right)\right), \tag{2.1}$$

where $k_{10} = 0.3116\,\mathrm{W\,m^{-1}\,K^{-1}}$ is the conductivity at room temperature $T_0 \approx 300\,\mathrm{K}$, and $\gamma = 0.275$ is the conductivity variation parameter.

The normal thermal conductivity of melted glass is about $k_2 = 0.7\,\mathrm{W\,m^{-1}\,K^{-1}}$, and is only weakly dependent on the temperature. However, the effect of the multiple

https://doi.org/10.1017/S1446181115000206 Published online by Cambridge University Press

reflections and absorptions in the reacting batch layer significantly increases the heat transfer through this layer. It can be shown (see Rosseland [6] or Siegel and Howell [9]) that the net effect of multiple reflections is to greatly enhance the thermal conductivity from its molecular value k_2 by a temperature-dependent radiation term to give an effective conductivity

$$k_{2\,\mathrm{eff}} = k_2 + k_{2\,\mathrm{rad}} \gg k_2 \quad \text{where } k_{2\,\mathrm{rad}} = \frac{16n^2}{3}\frac{\sigma T^3}{a_R}; \tag{2.2}$$

here n is the refractive index, a_R is an absorption coefficient calculated from the spectral absorption of the glass melt, and σ is the Stefan–Boltzmann constant. Using numerical semi-transparent model simulations, Wu and Viskanta [11] obtained fitted results for $k_{2\,\mathrm{eff}}(T)$, giving the quadratic approximation

$$k_{2\,\mathrm{eff}} = 5.39 - 0.0217 \times T + 0.0000206 \times T^2, \tag{2.3}$$

which we write in a more useful form

$$k_{2\,\mathrm{eff}} = k_{2m}[1 - \alpha(T - T_m) + \beta(T - T_m)^2],$$

where $k_{2m} \approx 7$ is identified as the conductivity of the just-melted batch. Over the temperature range of interest, from melting T_m (1123 K) to the gas temperature T_g (1850 K), this quadratic function exhibits a negligible difference from the theoretical cubic result (2.2). Moreover, the small value of the coefficient β suggests that a linear approximation would be almost as good, and adopting this even simpler form leads to some explicit analytic results.

We have already indicated that the radiative term $F(z, t)$ is somewhat intricate, and indeed, it involves incident, emission and absorption integrals with respect to wavelength and over the partially converted melt depth. Furthermore, both $F(z, t)$ and the enthalpy term $H_2(z, t)$ depend on the fraction of the melt f_b that is yet to be converted. It is possible to avoid a detailed determination of $f_b(z, t)$ by making the assumption that one can identify a temperature range ΔT_m over which melting occurs and thereby associate a fractional melting temperature T_f with each f_b. Explicitly,

$$f_b = f_{b0} + (1 - f_{b0})\frac{T_f - T_m}{\Delta T_m}$$

with $\Delta T_m \approx 250$ K. Even with this simplification, the analysis is daunting and parameter estimation is somewhat problematic.

Wu and Viskanta [11] obtained numerical solutions of the above system for batch elements of depth between 2 and 4 cm. They predicted overall melting times of between 130 and 350 s, broadly consistent with observations. One difficulty associated with the interpretation of these numerical simulations is to know how sensitive the results may be to the parameter values used, especially when it is remembered that some of these are at best only poorly estimated. It is with this background that our aim is to simplify the model further while preserving the important aspects of the melting of the batch.

https://doi.org/10.1017/S1446181115000206 Published online by Cambridge University Press

As it is not immediately obvious what is the most appropriate way to tackle our problem, it is helpful to first examine some of the timescales involved. Sand is a poor conductor, so one would expect the time required to raise the surface of the batch to the melting point T_m to be relatively small. Classical theory [2] tells us that the rise in the surface temperature of a semi-infinite body of conductivity k_1 due to a constant heat flux q into the surface is

$$T_h = \frac{q}{\sqrt{\pi \rho_1 c_1 k_1}} \sqrt{t}.$$

In our case, if we take the heat input as being due solely to flame radiation, this implies that $q = \varepsilon \sigma T_R^4$ where $\varepsilon \approx 0.7$ is the emissivity. This then gives a pre-melting timescale of some 8–20 s depending on the choice of k_1 within the range given by (2.1). These values are very much less than the melting time of the batch. Of course, the bottom of the batch layer is in direct contact with the molten glass in the furnace at temperature $T_b \approx 1500$ K, so melting will be immediately initiated on the underside of the batch.

Conduction timescales can be estimated by noting that in the absence of melting the time required for heat to conduct through a layer of thickness h is approximately

$$t_1 = h^2/\kappa_1 \quad \text{where } \kappa_1 \equiv k_1/(\rho_1 c_1). \tag{2.4}$$

Since the conductivity of sand increases from 0.35 to 0.66 W m^{-1} K^{-1} over the temperature range of interest, this suggests a conduction time of some 15–30 min for a 2 cm layer. This is significantly longer than the observed time for melting (130–350 s), so conduction through sand can be ruled out as a controlling factor of the overall melting process. If we consider the molten silica glass (zone 2) and the effective k_2 given by (2.3), then the molten batch behaves as a good conductor owing to radiative exchanges.

Last, we consider the expected melting time should radiation alone provide the latent heat to melt the batch. In this case, the time required would be

$$t_R = \frac{\rho_1 (\Delta h_m) h}{\varepsilon \sigma (T_R^4 - T_m^4)}, \tag{2.5}$$

where Δh_m is the latent heat per unit mass required to convert sand into molten glass. In writing down t_R the re-radiation from the front at the melting temperature T_m has been accounted for. With characteristic values this formula implies a melting time of some 30–50 s for a 2 cm batch layer. Moreover, since both the radiative input from the flames and the conductive and convective heat transfer from the gas in contact with the batch help to melt it, the dimensionless grouping

$$\mathcal{K} = \frac{k_{2\,\mathrm{eff}}(T_g - T_m)}{\varepsilon \sigma (T_R^4 - T_m^4) h}$$

provides a useful measure for the comparative size of these heat inputs. We will, henceforth, refer to $\mathcal{K}$ as the *convective heat transfer parameter.* For a 4 cm batch

https://doi.org/10.1017/S1446181115000206 Published online by Cambridge University Press

layer, using a range of values for $k_{2\,\mathrm{eff}}$ gives $\mathcal{K}$ in the range 0.2–1.1 for typical gas temperatures. It is clear from this that heat transfer through hot gas contact can be as large as the radiative heat input.

Of major importance for the melting process is the ratio of the heat required to raise the temperature of the batch from its initial value T_0 to the melting temperature T_m, to the latent heat required to melt the batch, a ratio referred to as the *Stefan number*. Using the parameters above (and ignoring the heat required to dry the batch), we find that

$$\mathcal{S} = \frac{c_1(T_m - T_0)}{\Delta h_m} \approx 1.6,$$

which indicates that the sensible and latent heat requirements for the melting process are of similar sizes.

We conclude from the above that the effect of multiple reflections within the melting batch is to greatly increase the conductivity of the melt and thus significantly reduce the expected melting time from about 1 h down to a few minutes. One would expect the speed of the front to be much greater than the solid batch conduction speed and also somewhat larger than the radiative melting speed. These observations motivate the simplified system that is presented below.

2.1. The simplified model We develop our model by assuming that all absorption and melting occurs in the vicinity of the front $z = s(t)$, so that completely melted glass lies above an unconverted batch below. Under such circumstances the appropriate condition to impose at the front is the *Stefan condition*

$$\varepsilon\sigma(T_R^4 - T_m^4) + q_{1s} - q_{2s} = -\rho_1 \Delta h_m \frac{ds}{dt}, \tag{2.6}$$

where $q_{2s} = -k_{2\,\mathrm{eff}}(T_m)(\partial T_2/\partial z)$ is the heat flux from the front into the molten batch, and $q_{1s} = -k_1(T_m)(\partial T_1/\partial z)$ is the heat flux from the unconverted batch into the front (see Figure 2). Furthermore, the front must be at the melting temperature T_m which necessitates the continuity condition

$$T_1(z,t) = T_2(z,t) = T_m \quad \text{at } z = s(t). \tag{2.7}$$

The Rosseland approximation (2.2) is a simplification of the radiative transport equation for optically thick media, and with this enforced and local latent heat terms relegated to the melting front, the heat equation in the melt (zone 2) becomes

$$\rho_2 c_2\left[\frac{\partial T_2}{\partial t} + \left\{\left(1 - \frac{\rho_1}{\rho_2}\right)\frac{ds}{dt}\frac{\partial T_2}{\partial z}\right\}\right] = \frac{\partial}{\partial z}\left(k_{2\mathrm{eff}}(T)\frac{\partial T_2}{\partial z}\right) \quad \text{for } z > s(t), \tag{2.8}$$

while the equation in the unmelted batch remains

$$\rho_1 c_1 \frac{\partial T_1}{\partial t} = \frac{\partial}{\partial z}\left(k_1(T)\frac{\partial T_1}{\partial z}\right) \quad \text{for } z < s(t). \tag{2.9}$$

To complete the specification of the problem, we need to describe the heat exchange between the melt and the gas at temperature T_g. This is modelled by a Robin condition

$$q_{2h} = -k_{2\,\mathrm{eff}}(T_h(t))\frac{\partial T_2(h)}{\partial z} = \mu(T_h(t) - T_g), \tag{2.10}$$

https://doi.org/10.1017/S1446181115000206 Published online by Cambridge University Press

where $T_h(t) = T_2(h,t)$ is identified as the surface temperature of the melt, q_{2h} is the heat flux through the surface of the melt and μ is the heat transfer coefficient. The gas temperature T_g is determined by the furnace geometry and global heat conservation considerations, but for present purposes it is sufficient to suppose that T_g is prescribed and may be adjusted by suitable modifications to the furnace, for example, by altering the gap between the molten glass and the flame.

This completes the specification of our problem. To summarize, above and below the front $z = s(t)$, equations (2.8) and (2.9) respectively hold, and across the front the continuity of temperature (2.7) and the Stefan law (2.6) apply. Given these simplifications, let us now seek an appropriate quasi-steady solution structure that describes the melting process with a slowly moving front.

3. Quasi-steady solution

It is convenient to begin our study of the process with the melting zone 2 lying above the front. It is helpful to nondimensionalize lengths on the batch depth h and express time in terms of the radiation timescale t_R defined in (2.5). Thus, we define $t = t_R\widetilde{t}$ and write the temperature of the batch material

$$T_2 = T_m + (T_g - T_m)\widetilde{T}_2,$$

so that $T_2 = T_m$ and $T_2 = T_g$ correspond to $\widetilde{T}_2 = 0$ and 1, respectively. Furthermore, the input flux at the top of the batch is scaled on $\mu(T_g - T_m)$ and the conductivity on its effective value $k_{2m} \equiv k_{2\,\mathrm{eff}}(T_m)$ at the melting temperature. Consequently, we introduce dimensionless flux and conductivity variables $\widetilde{q}_{2h}$ and $\widetilde{k}_2$ as

$$q_{2h} = \mu(T_g - T_m)\widetilde{q}_{2h} \quad \text{and} \quad k_{2\,\mathrm{eff}}(T_2) = k_{2m}\widetilde{k}_2(\widetilde{T}_2).$$

Assuming a quasi-steady profile and ignoring volumetric changes, the heat equation (2.8) reduces to

$$\frac{\partial}{\partial z}\left[\widetilde{k}_2(\widetilde{T}_2)\frac{\partial \widetilde{T}_2}{\partial z}\right] = 0,$$

and an integration followed by application of the surface condition (2.10) gives

$$-\widetilde{k}_2(\widetilde{T}_2)\frac{\partial \widetilde{T}_2}{\partial z} = \widetilde{T}_h - 1,$$

where $\widetilde{T}_h$ is the scaled surface temperature which is yet to be determined. A second integration and imposition of the requirement that $\widetilde{T}_2 \to 0$ at the melting front $z = s(\widetilde{t})$ yields

$$\int_0^{\widetilde{T}_2} \widetilde{k}_2(w)\,dw = (\widetilde{T}_h - 1)(s(\widetilde{t}) - z).$$

This equation implicitly determines the temperature field $\widetilde{T}_2(z)$ through the melt; necessarily $\widetilde{T}_2(1) = \widetilde{T}_h$, thereby requiring

$$\int_0^{\widetilde{T}_h} \widetilde{k}_2(w)\,dw = (\widetilde{T}_h - 1)(s(\widetilde{t}) - 1), \tag{3.1}$$

which can be solved for $\widetilde{T}_h$ for any prescribed $\widetilde{k}_2(\widetilde{T}_2)$.

https://doi.org/10.1017/S1446181115000206 Published online by Cambridge University Press

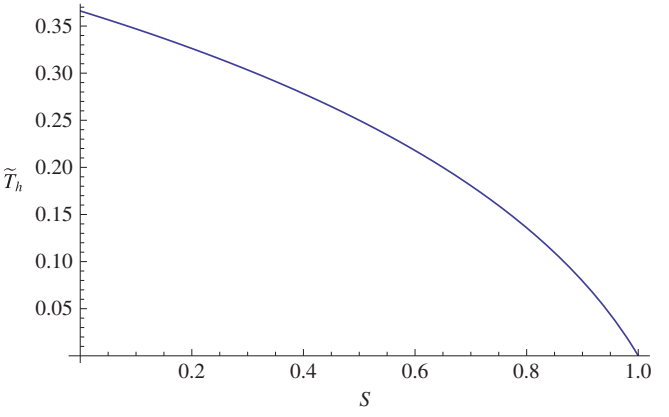

FIGURE 3. The scaled surface temperature of the melt as a function of the (scaled) location $s(\widetilde{t})$. Result corresponding to a gas temperature of 1850 K.

As was noted earlier in our discussion of (2.3), the tiny coefficient of the quadratic term means that the variation of the conductivity over the temperature range is virtually linear, so with minimal error we may write

$$\widetilde{k}_2(\widetilde{T}_2) = 1 + \widetilde{T}_2(\widetilde{k}_{2g} - 1),$$

where $\widetilde{k}_{2g} \equiv \widetilde{k}_2(1)$ is the scaled conductivity of the melt at the gas temperature. The consistency result (3.1) then gives

$$\widetilde{T}_h + \tfrac{1}{2}(\widetilde{k}_{2g} - 1)(\widetilde{T}_h)^2 = (\widetilde{T}_h - 1)(s(\widetilde{t}) - 1),$$

so that the surface temperature and associated heat flux are, respectively,

$$\widetilde{T}_h = \frac{1}{(\widetilde{k}_{2g} - 1)}\left[\sqrt{1 + (1 - s)\left\{2\widetilde{k}_{2g} + 1 - s\right\}} - 2 + s\right] \quad \text{and} \quad \widetilde{q}_{2h} = (\widetilde{T}_h - 1).$$

Figure 3 displays the scaled surface temperature $\widetilde{T}_h$ as a function of the location of the front position s. Note that initially the temperature of the surface is T_m (so $\widetilde{T}_2 = 0$), and it gradually increases to values closer to the gas temperature as melting proceeds towards completion as $s \to 0$. It is also noted that $\widetilde{q}_{2h} < 0$, so that heat from the combustion gases assists the melting of the batch.

Now we turn to the unmelted zone 1. Although we continue to scale lengths and times in the same way as was used for zone 2, here it is convenient to adopt an alternative notation for the temperature and the conductivity. The temperature of the batch is written using the room temperature as the reference base, so that

$$T_1 = T_0 + (T_m - T_0)\widehat{T}_1(z, \widetilde{t}).$$

With this form of the temperature, the definition (2.1) for the conductivity can be cast as $k_1 = k_{10}\exp(\gamma_0\widehat{T}_1)$ with $\gamma_0 \equiv \gamma(T_m - T_0)/T_0$. Furthermore, it is helpful to scale the

https://doi.org/10.1017/S1446181115000206 Published online by Cambridge University Press

flux from the unconverted batch into the front, so that

$$q_1 = \left[\frac{k_{10}(T_m - T_0)}{h}\right]\widehat{q}_1 \quad \text{with } \widehat{q}_1 = -\exp(\gamma_0\widehat{T}_1)\frac{\partial \widehat{T}_1}{\partial z}.$$

We seek a travelling wave solution of the form $\widehat{T}_1 = \widehat{T}_1(\zeta)$ with $\zeta \equiv s(\widetilde{t}) - z$, subject to $\widehat{T}_1(0) = 1$ and $\widehat{T}_1(\infty) = 0$. These boundary conditions reflect the expectation that the temperature $T_1 = T_m$ at the front, and it approaches the room temperature of the batch far from the front. If this ansatz is substituted in the unmelted batch equation (2.9) and the scalings applied, the result is

$$\lambda\dot{s}\frac{\partial \widehat{T}_1}{\partial \zeta} = \frac{\partial}{\partial \zeta}\left(\exp(\gamma_0\widehat{T}_1)\frac{\partial \widehat{T}_1}{\partial \zeta}\right) \quad \text{with } \lambda = \left[\frac{h^2\rho_1 c_1}{k_{10}t_R}\right] \equiv \frac{t_1}{t_R}, \tag{3.2}$$

where $\dot{s}$ is the front speed. Note that the parameter λ is the ratio of the conduction t_1 (2.4) and radiation t_R (2.5) timescales, which is expected to be large. Integration of equation (3.2) yields

$$\lambda\dot{s}\widehat{T}_1 = \exp(\gamma_0\widehat{T}_1)\frac{\partial \widehat{T}_1}{\partial \zeta}, \tag{3.3}$$

which requires that $\widehat{T}_1 \to 0$ as $\zeta \to \infty$. Evaluating this at the front $\zeta = 0$, where $\widehat{T}_1 = 1$, gives

$$\lambda\dot{s} = -\widehat{q}_1(0) \equiv -\widehat{q}_{1s},$$

so the unscaled heat input from the front into the unconverted batch is given by

$$-q_{1s} = -\left[\frac{k_{10}(T_m - T_0)}{h}\right]\lambda\dot{s} \equiv -\left[\frac{h\rho_1 c_1(T_m - T_0)}{t_R}\right]\dot{s}$$

using (3.2). This result simply states that the sensible heat input ($-q_{1s}$) required to raise the temperature of sand to the melting temperature needs to be supplied by conduction from the front.

Equation (3.3) can be integrated again to give

$$-\lambda\dot{s}\zeta = \mathrm{Ei}(\gamma_0\widehat{T}_1) - \mathrm{Ei}(\gamma_0), \tag{3.4}$$

where Ei is the exponential integral function defined by $\mathrm{Ei}(x) \equiv \int_{-\infty}^{x} t^{-1}e^t\,dt$ in which the integral is taken to be the Cauchy principal value. For small $\widehat{T}_1$, this solution is given by $\widehat{T}_1 \approx \exp(-\lambda\dot{s}\zeta)$, so heat from the travelling front penetrates a scaled distance of order $\lambda^{-1} \ll 1$ into the unreacted batch. Translated into dimensional terms, and using the characteristic parameter values cited earlier, this suggests that for batch depths of 2–4 cm, the penetration length is roughly 5% of the batch height.

The temperature variation through the melting front as given by the solution of (3.4) is depicted in Figure 4. The thermal profile is strongly dependent on the value of the conductivity variation parameter γ_0 ($= \gamma(T_m - T_0)/T_0$). We remark that $\gamma_0 \approx 0.75$ for an input batch temperature of 300 K, and it increases as T_0 decreases. The temperature profile becomes sharper and thins as the batch input temperature grows, with the

https://doi.org/10.1017/S1446181115000206 Published online by Cambridge University Press

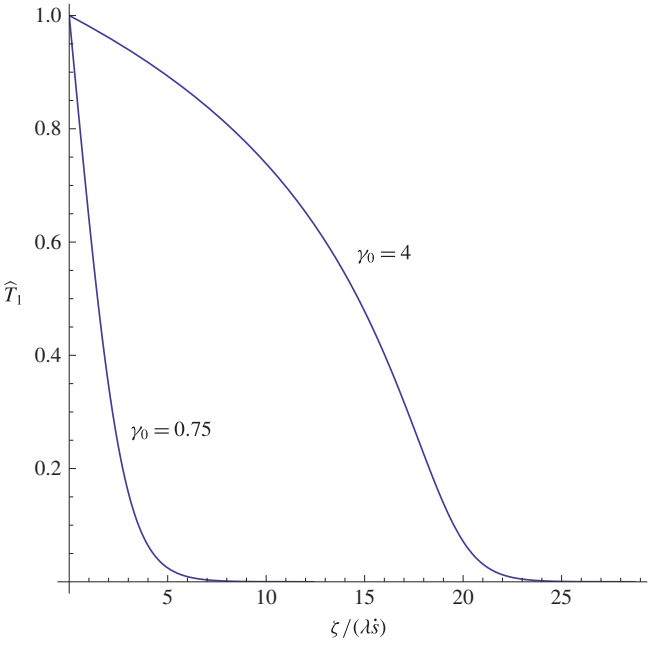

FIGURE 4. The scaled temperature variation $\widehat{T}_1(\zeta)$ through the front for the two cases $\gamma_0 = 0.75$ and $\gamma_0 = 4$.

consequence that pre-heating a batch could significantly affect the heating history of a particle.

Having modelled the various components of heat transfer into and out of the front, what remains is the issue of the propagation speed of the front. This is settled by examination of the Stefan condition (2.6) which, when cast in terms of the dimensionless quantities, becomes

$$[\mu(T_g - T_m)](\widetilde{T}_h - 1) - \left[\frac{h\rho_1 c_1(T_m - T_0)}{t_R}\right]\dot{s} = [\varepsilon\sigma(T_R^4 - T_m^4)] + \left[\frac{\rho_1 \Delta h_m h}{t_R}\right]\dot{s}.$$

On recalling the definition of the radiative timescale t_R given by (2.5), this reduces to the ordinary differential equation

$$(1 + \mathcal{S})\frac{ds}{d\widetilde{t}} = -1 + \mathcal{K}(\widetilde{T}_h - 1), \tag{3.5}$$

which depends on the Stefan number $\mathcal{S}$ and the convective heat transfer parameter $\mathcal{K}$. If it is recalled that the time has been scaled using t_R, then further simplification can be achieved by adopting the melting timescale $t_m = (1 + \mathcal{S})t_R$. If $\widetilde{t} = (1 + \mathcal{S})t^\dagger$, then

$$\frac{ds}{dt^\dagger} = -1 + \mathcal{K}(\widetilde{T}_h(s) - 1),$$

which is a separable equation for $s(t^\dagger)$. We have previously noted that for realistic values, $\mathcal{K}$ probably lies in the range between 0.2 and 1.1, with its precise value

https://doi.org/10.1017/S1446181115000206 Published online by Cambridge University Press

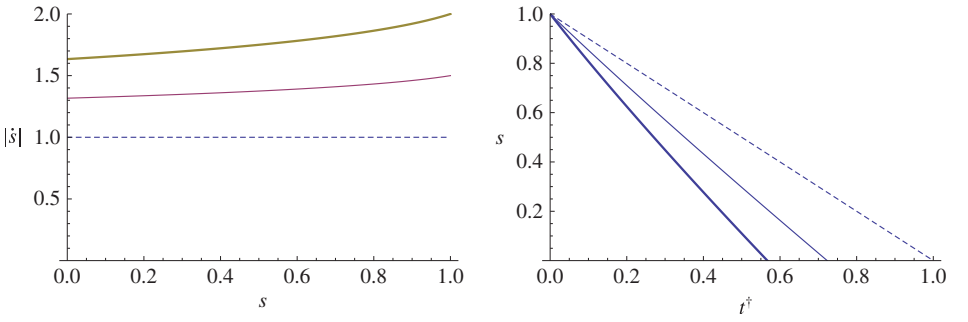

FIGURE 5. Movement of the front for the three values, $\mathcal{K} = 0, 0.5$ and 1 (dashed, thin and thick lines, respectively). The left-hand plot shows the scaled front speed $|\dot{s}|$ as a function of location s within the batch. The right-hand plot illustrates the evolution of the front location s as a function of scaled time $t^\dagger$.

depending on the combustion gas and effective radiation temperatures. Plots of the front speed $\dot{s}$ as a function of front location s and of this position as a function of $t^\dagger$ are given in Figure 5. When $\mathcal{K} = 0$ there is no heat transfer from the combustion gases, so that the front travels with constant speed, and the melting time is $t_m = t_R$. Increasing the value of $\mathcal{K}$ corresponds to additional convective transfer from the combustion gases, and the melting time almost halves due to convective heat transfer from the hot gas. The implication is that reducing the depth of the furnace can significantly reduce the batch melting time.

We also note that when $\mathcal{K} \neq 0$ the front speed falls slightly as melting proceeds due to the changed effective conductivity of the melt. A useful approximation can be obtained by simply averaging the right-hand side of (3.5) to give the constant front speed of

$$\left|\frac{ds}{dt^\dagger}\right| = \frac{1 + \mathcal{K}\mathcal{F}(\widetilde{k}_{2g})}{1 + \mathcal{S}}, \tag{3.6}$$

where

$$\mathcal{F}(\widetilde{k}_{2g}) = 1 + \frac{1}{2(\widetilde{k}_{2g} - 1)}\left[\left(\sqrt{2 + 2\widetilde{k}_{2g}} + \sqrt{1 + 2\widetilde{k}_{2g}}\right) - 3\right],$$

which implies that the effect of combustion gas on front speed is to increase it by the factor $1 + \mathcal{K}\mathcal{F}(\widetilde{k}_{2g})$.

4. Discussion and closing comments

The quantitative results obtained in this work complement the numerical simulations previously obtained by Wu and Viskanta [11], but the results have the advantage of being both relatively simple and explicit, and thus can provide better understanding of the important processes involved. An appreciation of the key parts of the complicated process of glass manufacture could enable quick operational adjustments to be made on-site. Some of the highlights of our findings include the

https://doi.org/10.1017/S1446181115000206 Published online by Cambridge University Press

observation that the front speed through the melt seems to remain almost constant, and that the heat transfer from the gas may have a profound effect on this progression. An adjustment to the spacing between the flames and the batch can significantly affect the melting time, as can an increase in the radiative input.

In this model we have neglected the lower front that can be expected to move upwards through the batch. Since the bottom of the batch is in contact with melted glass at a temperature greater than the melting point T_m, we would anticipate some melting upwards. The temperature variations under the batch as it moves into the furnace are relatively small, so that the heat transfer driving the lower front will remain almost constant and the front speed is given by

$$\dot{s_b} = \mu_1 \frac{(T_b - T_m)}{\rho_2 \Delta h_m},$$

where μ_1 is the heat transfer coefficient. This front progresses relatively slowly compared with the radiation-driven upper front and would be best measured or inferred from observations. The temperature profile near this front is the same as that obtained for the upper one; importantly, its thickness is small, and so the two fronts act almost independently until they begin to overlap and interfere with each other. Theoretically it should be possible to quantify this late stage of melting, but in our context such a calculation would be completely academic and of no practical value since melting is essentially complete once the fronts begin to merge.

The simplest possible model for the melting process would assume a direct transfer of radiating heat from the flames to the melting front while ignoring conductive heat transfer through the melt. This corresponds to the $\mathcal{K} = 0$ limit of our melting speed result (see (3.6)). However, we have seen that convective (or conductive) heat transfer from the gas in contact with the batch surface, through the partially melted and fizzing (due to bubbles) melt, modifies this result by a multiplicative factor $1 + \mathcal{K}\mathcal{F}$. Somewhat surprisingly, for typical practical input parameter values, the front speed still remains reasonably constant as the front progresses through the batch, even though the variations of surface temperature of the melt are quite large; see Figure 3.

We admit that there are many uncertainties not accounted for in this simple model; for example, the Rosseland model (2.3) assumes a uniform distribution of scattering points. Furthermore, practice batches consist of piles of material, rather than a uniform depth layer as used in the model developed in this paper, and this might be significant since the available batch surface area exposed to radiation will change near the end of the melting process. Despite these obvious shortcomings, our analysis has identified the important dimensionless groups $\mathcal{S}$ and $\mathcal{K}$. Experimental tuning should result in minor modifications of the results obtained, and plausibly provide a useful basis for furnace control and design. Variations in batch properties can arise due to changed sourcing or climatic conditions, and it is evident that different glasses require different batch compositions. From the glass quality point of view, the thermal history of batch particles determines the propensity of the batch to retain or shed bubbles of various sizes into the molten glass bath, so the melting layer thermal structure results are likely to be useful.

https://doi.org/10.1017/S1446181115000206 Published online by Cambridge University Press

Our modelling here has been concerned with the physical mechanism of the production of glass at the exclusion of many of the chemical aspects of the problem. Flaws (often bubbles) are always present in plate glass, and if they are sufficiently large, can unacceptably corrupt its optical integrity. Sheets that are compromised in this way have to be recycled, which is an unnecessary expense. The bubbles originate from within the furnace, and some preliminary work on the formation, growth and movement of bubbles within a furnace has been done. We hope to report the outcomes of this work in due course.

Acknowledgements

This work was commenced at the Mathematics in Industry Study Group held in South Africa during 2013. The outcomes of that workshop are to be found in [5]. While many contributed to the work on this glass problem, particular gratitude is expressed to the industrial representative Eddie Ferreira from PFG who provided exceptional information and guidance during the meeting.

References

[1] O. Auchet, P. Riedinger, O. Malasse and C. Iung, "First-principles simplified modelling of glass furnaces combustion chambers", *Control Engineering Practice* **16** (2008) 1443–1456; doi:10.1016/j.conengprac.2008.04.005.

[2] H. S. Carslaw and J. C. Jaeger, *Conduction of heat in solids* (Oxford University Press, Oxford, 1959).

[3] P. D. Howell, "Extensional thin layer flows", Ph.D. Thesis, St Catherines College Oxford, 1994, http://eprints.maths.ox.ac.uk/25/1/howell.pdf.

[4] E. Le Bourhis, *Glass: mechanics and technology* (Wiley-VCH, Weinheim, 2008).

[5] Proceedings of South African Maths in Industry Study Group, 2013, http://www.wits.ac.za/newsroom/21966/outcomes.html.

[6] S. Rosseland, *Theoretical astrophysics* (Clarendon Press, Oxford, 1936).

[7] V. Schick, B. Remy, A. Degiovanni and F. Demeurie, "Measurement of thermal conductivity of liquids at high temperature", *J. Phys: Conf. Ser.* **395** (2012) Article 012078; doi:10.1088/1742-6596/395/1/012078. 6th European Thermal Sciences Conference (Eurotherm 2012).

[8] H. Shibata, A. Suzuki and H. Ohta, "Measurement of thermal transport properties for molten silicate glasses at high temperatures by means of a novel laser flash technique", *Mater. Trans.* **46** (2005) 1877–1881; doi:10.2320/matertrans.46.1877.

[9] R. Siegel and J. R. Howell, *Thermal radiation heat transfer*, 4th edn (Taylor & Francis, London, 2002).

[10] F. V. Tooley, *The handbook of glass manufacture, books for industry* (Ashlee Publishing, New York, 1974).

[11] X. Wu and R. Viskanta, "Modelling of heat transfer in the melting of a glass batch", *J. Non-Crystaline Solids* **80** (1986) 613–622; doi:10.1016/0022-3093(86)90454-0.